

EVALUATION OF THE CRYSTALLISATION KINETICS OF POLY(PROPYLENE TEREPHTHALATE) USING DSC AND POLARIZED LIGHT MICROSCOPY*

D. S. Achilias**, G. Z. Papageorgiou and G. P. Karayannidis

Laboratory of Organic Chemical Technology, Department of Chemistry, Aristotle University of Thessaloniki
54124 Thessaloniki, Greece

In this study, isothermal crystallisation kinetic data of poly(propylene terephthalate) (PPT) are obtained using differential scanning calorimetry (DSC) and polarized light microscopy (PLM). Data from each method are analyzed according to the secondary nucleation theory of Lauritzen–Hoffmann and the procedures and results are critically presented. The assumption that the growth rates obtained from PLM can be equally well described from crystallisation rate data using the half-crystallisation time, is tested.

Keywords: crystallisation kinetics, DSC, PLM, poly(propylene terephthalate)

Introduction

Crystallisation kinetics is crucial in polymer processing, since it determines the resulting morphology, as well as the degree of crystallinity and consequently the properties (mechanical, thermal, etc.) of the final polymer products. Thermal analysis methods such as DSC or PLM are usually used to study crystallisation kinetics of polymers. DSC can be used to obtain both isothermal and nonisothermal crystallisation data, while PLM is mainly used for isothermal crystallisation experiments. DSC is a macroscopic method in which the overall rate of the phenomenon can be measured. In contrast, using PLM, which is a rather microscopic method, the spherulite growth rate can be measured directly. However, PLM cannot be used in cases of polymers, which form only small spherulites and thus limiting its applicability.

One of the most widely accepted theories describing the temperature dependence of the growth rate measure microscopically, is the Lauritzen–Hoffmann theory [1, 2]. The major application area of this theory is polymer crystallisation under isothermal conditions, while it has also been used under non-isothermal conditions [3]. Accordingly, the growth rate, G , is given as a function of the crystallisation temperature, T_c , by the following bi-exponential equation:

$$G = G_0 \exp\left[-\frac{U^*}{R(T_c - T_\infty)}\right] \exp\left[-\frac{K_g}{T_c(\Delta T)f}\right] \quad (1)$$

where G_0 is the pre-exponential factor, the first exponential term contains the contribution of diffusion pro-

cess to the growth rate, while the second exponential term is the contribution of the nucleation process; U^* denotes the activation energy which characterizes molecular diffusion across the interfacial boundary between melt and crystals and T_∞ is set equal to $(T_g - 30)$ K; K_g is a nucleation constant and ΔT denotes the degree of undercooling ($\Delta T = T_m^0 - T_c$); f is a correction factor which is close to unity at high temperatures and is given as $f = 2T_c / (T_m^0 + T_c)$; the equilibrium melting temperature, T_m^0 can be calculated using some extrapolative procedure like the linear or nonlinear Hoffman–Weeks extrapolation. For a secondary or heterogeneous nucleation, K_g can be calculated from:

$$K_g = \frac{m\sigma_e b_0 T_m^0}{\Delta h_f \rho_c k_B} \quad (2)$$

where m takes the value of 4 when crystallisation takes place in regimes I or III and the value 2 in regime II, σ , σ_e are the side surface (lateral) and fold surface free energies which measure the work required to create a new surface, b_0 is the single layer thickness, $\Delta h_f \rho_c = \Delta H_f$ is the enthalpy of melting per unit volume and k_B is the Boltzmann constant.

The nucleation parameter, K_g , can be calculated from Eq. (1) using the double logarithmic transformation:

$$\ln G + \frac{U^*}{R(T_c - T_\infty)} = \ln G_0 - \frac{K_g}{T_c(\Delta T)f} \quad (3)$$

Plotting the left-hand side of Eq. (3) with respect to $1/[T_c(\Delta T)f]$ a straight line should appear having a slope equal to K_g . Critical break points, identified by

* Presented at MEDICTA 2005 Conference, Thessaloniki, peer reviewed paper.

** Author for correspondence: axilias@chem.auth.gr

the change in the slope of the line, when appear in such a plot, have been attributed to regime transitions accompanied by morphological changes of the crystals formed (i.e. change from axialite-like to banded spherulite and non-banded spherulite morphology). According to Eq. (2) the theoretical ratio of $K_{g(III)}/K_{g(II)}$ should be equal to 2.

In Eq. (3), normally G is calculated from PLM data [4]. However, several authors have treated the isothermal crystallisation rate data obtained by DSC, according to the Lauritzen–Hoffmann analysis (Eq. (3)) and assumed that G is proportional to the inverse of the crystallisation half time ($G \approx 1/t_{1/2}$) [5–9]. The validity of such an attempt has not been tested yet [10].

In this study, this modification against the microscopically measured growth rates is critically examined. Both, PLM and DSC isothermal crystallisation experiments on the same polymer were carried out. The applicability of the Lauritzen–Hoffman treatment in both cases of data collected during PLM but also DSC experiments is critically presented. Poly(propylene terephthalate) (PPT) has been selected as a model polymer, not extensively studied in literature. Isothermal crystallisations were performed at various temperatures from values close to the melting point until large undercoolings. Three different PPT resins were examined having different average molecular masses.

Experimental

Details on the PPT synthesis can be found in [11]. In this investigation, three PPT resins were used given the code names PPT-0.69, PPT-0.40 and PPT-No according to [12], denoting samples with intrinsic viscosities 0.69, 0.40 and 0.36 dL g⁻¹, respectively. From these values the mass average molecular mass of each sample was calculated to be 32100, 14600 and 12500, respectively.

All crystallisation experiments were performed in a PerkinElmer, Pyris 1 differential scanning calorimeter. The instrument was calibrated using high purity indium and zinc standards. Samples of about 5 mg were used. Isothermal crystallisation tests were performed at a temperature range from 182 to 209°C. The samples, sealed in aluminum pans, were initially melted at 270°C for 5 min to erase all previous thermal history, and then cooled to the desired crystallisation temperature at a rate of 100°C min⁻¹. A fresh sample was used in each test. Tests were performed under a nitrogen atmosphere and melting for only 5 min was allowed to prevent thermal degradation of the polyesters.

Measurement of the radius growth rate of PPT crystallites under isothermal crystallisation was investigated using a Polarizing Light Microscope (PLM)

(Nikon, Optiphot-2) equipped with a Linkam THMS 600 heating stage and a TP 91 control unit. Heating rates were 10°C min⁻¹. Microphotographs were taken using a JVC TM-1500 E (CV) colour video monitor and a Sony UP-1200 AEP video printer. For the crystallisation experiments the conditions were very similar as for the DSC ones, i.e. the samples were initially melted to 270°C for 5 min, rapidly cooled to the crystallisation temperature at a rate of 100°C min⁻¹ and then held at that temperature to crystallize. The subsequent growth of a particularly selected PPT spherulite was viewed between crossed polars and recorded by a video camera at appropriate time intervals. By plotting crystal radius vs. time, the slope of the line, or the spherulitic growth rate G at different temperatures (182–209°C) can be obtained.

Results and discussion

PLM micrographs of PPT-0.69 sample isothermally crystallized from the melt appear in Figs 1 and 2 for various time intervals. At low crystallisation temperatures (182°C) spherulite morphology was observed, turned into an axialitic type at higher temperatures (215°C). The radius of crystallites increase with crystallisation time and such a plot at different crystallisation temperatures appear in Fig. 3. The solid lines represent the best least squares fit to the data. In all cases very good straight lines were observed. From the slopes of these lines the crystallite growth rate, G , was calculated. In the range of crystallisation temperatures studied, G decreased dramatically as the crystallisation temperature was increased.

Before kinetic analysis, it was important to estimate the values of U^* in Eq. (1). Usually, the empirical ‘universal’ value of $U^*=6280$ J mol⁻¹ (1500 cal mol⁻¹) is used [1]. Besides, a value of $U^*=17590$ J mol⁻¹ (4200 cal mol⁻¹) after Williams–Landel–Ferry (WLF) is

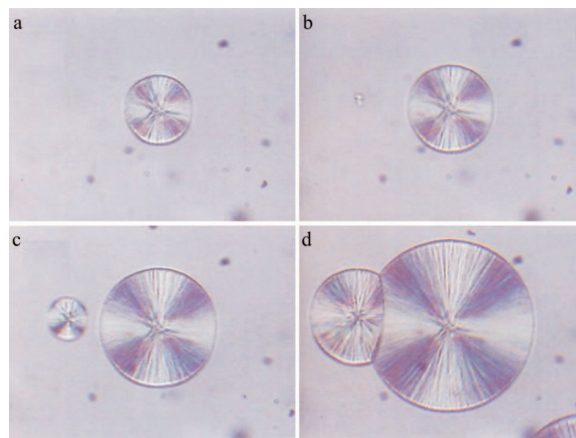


Fig. 1 PLM micrographs of PPT-0.69 crystallized at 182°C for various times: a – 15 s, b – 25 s, c – 35 s and d – 55 s

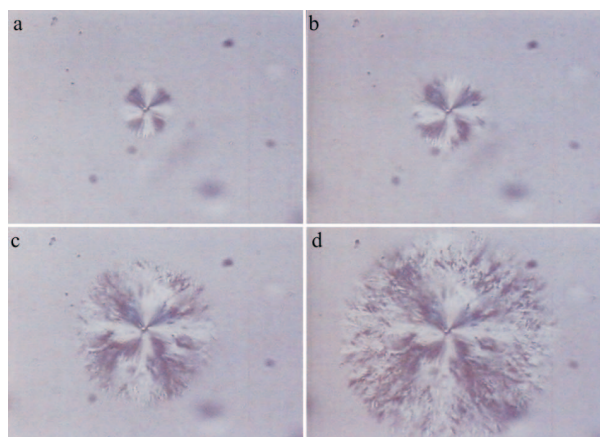


Fig. 2 PLM micrographs of PPT-0.69 crystallized at 215°C for various times: a – 15 s, b – 25 s, c – 35 s and d – 55 s

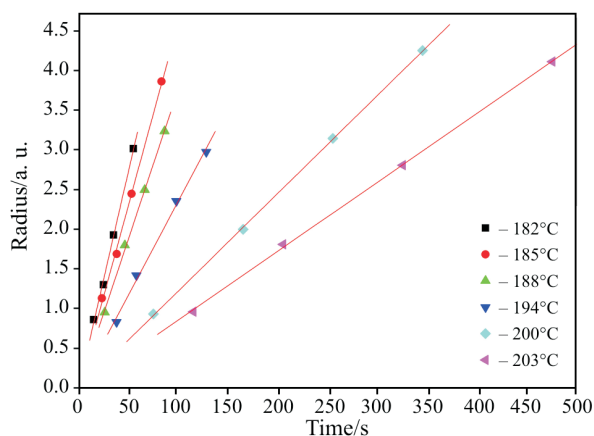


Fig. 3 Radius of crystallite as a function of time for different crystallisation temperatures

also employed [13]. In the present study, both the universal value of $U^*=6280 \text{ J mol}^{-1}$ and the WLF value of $U^*=17590 \text{ J mol}^{-1}$, together with an intermediate value of $U^*=12570 \text{ J mol}^{-1}$ ($3000 \text{ cal mol}^{-1}$) were examined. The objective was to study the influence of the chosen parameter on the determination of regime transitions and particularly on the ratio of the nucleation constant calculated in regime III over that in regime II. Figure 4 represents a Lauritzen–Hoffman type plot of PPT-0.69 at different U^* values. All curves show a clear break point at approximately 194°C denoting a crystallisation regime III→II transition at this temperature. Another break point is observed at approximately 215°C denoting a regime II→I transition in accordance to literature values [14]. Although the choice of the U^* value leads to the corresponding change in the line slopes, i.e. the values of nucleation constants $K_{g(\text{III})}$ and $K_{g(\text{II})}$, the regime III→II transition is always located at approximately the same temperature 194°C. The values of the nucleation constants calculated at different U^* values are listed in Table 1. It was found that the linear regression of the kinetic data for the two regimes (II and III)

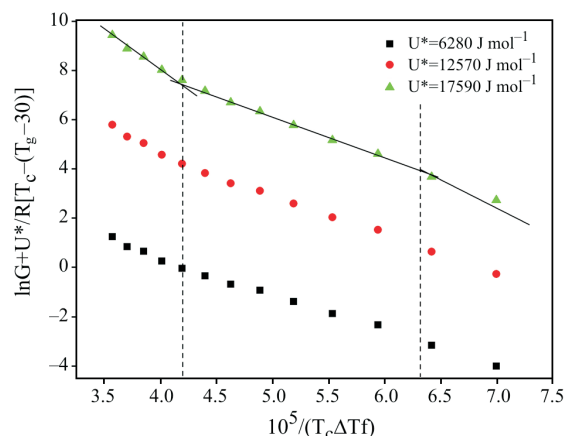


Fig. 4 Lauritzen–Hoffman type plots for PPT-0.69 for different values of U^*

are well at all different U^* values. However, when the value of U^* increased from 6280 to 17590 the ratio $K_{g(\text{III})}/K_{g(\text{II})}$ increased from 1.6 to 1.9 which is in the vicinity of the theoretical value 2. Thus, the value of $U^*=17590 \text{ J mol}^{-1}$ was used in this investigation.

Next, the other two PPT resins having different average molecular masses were analysed using PLM. The growth rate, G , calculated is presented in Fig. 5 in the form of Eq. (3). As it can be seen higher growth rates were observed when a resin with higher molecular mass was used. All curves show a break point at approximately 194°C denoting a crystallisation regime transition at this temperature for all three PPT resins. The nucleation parameters calculated for every resin are presented in Table 2. It was noticed that an increase of the average molecular mass led to lower K_g values and thus to lower surface free energies. The values calculated are approximately the same with corresponding reported in literature [15].

Furthermore, crystallisation of polymer melts usually releases significant amounts of heat, which can be measured by DSC. Based on the assumption that the evolution of crystallinity is linearly proportional to the evolution of heat released during the crystallisation, the relative crystallinity, $X(t)$, can be obtained. It has been assumed that the growth rate, G can be adequately described by the inverse half crystallisation time, i.e. $G \approx 1/t_{1/2}$ [5]. In this study, in order to check this assumption, several characteristic times were used, including the time to achieve 1% relative degree of crystallinity ($t_{0.01}$), 2% ($t_{0.02}$),

Table 1 Values of nucleation constants in regimes III and II for PPT-0.69 at various values of U^*

$U^*/\text{J mol}^{-1}$	$K_{g(\text{III})} 10^{-5}/\text{K}^2$	$K_{g(\text{II})} 10^{-5}/\text{K}^2$	$K_{g(\text{III})}/K_{g(\text{II})}$
6280	2.1	1.3	1.6
12570	2.7	1.5	1.8
17590	3.1	1.7	1.9

Table 2 Values of nucleation constants in regimes III and II for the three PPT samples

Sample	$K_{g(III)} 10^{-5}/K^2$	$K_{g(II)} 10^{-5}/K^2$	$K_{g(III)}/K_{g(II)}$	Reference
PPT-0.69	3.1	1.7	1.9	this study
PPT-0.40	3.2	1.9	1.7	this study
PPT-No	3.7	2.1	1.8	this study
PPT	3.0	1.4	2.1	[15]

Table 3 Nucleation parameters obtained using different characteristic times for the PPT-0.69 sample

Method used	$K_{g(III)} 10^{-5}/K^2$	$K_{g(II)} 10^{-5}/K^2$	$K_{g(III)}/K_{g(II)}$
DSC/ $G \approx 1/t_{1/2}$	3.5	2.5	1.4
DSC/ $G \approx 1/t_{0.10}$	3.7	2.5	1.5
DSC/ $G \approx 1/t_{0.05}$	4.0	2.5	1.6
DSC/ $G \approx 1/t_{0.02}$	4.5	2.4	1.9
DSC/ $G \approx 1/t_{0.01}$	4.9	2.3	2.1
DSC/ $G \approx (dX/dt)_{X=0.5}$	3.2	2.6	1.2

5% ($t_{0.05}$), 10% ($t_{0.10}$) and 50% ($t_{1/2}$). The results of using Eq. (3) with the assumption $G \approx 1/t$ and different values for t , are presented in Fig. 6. As it can be seen

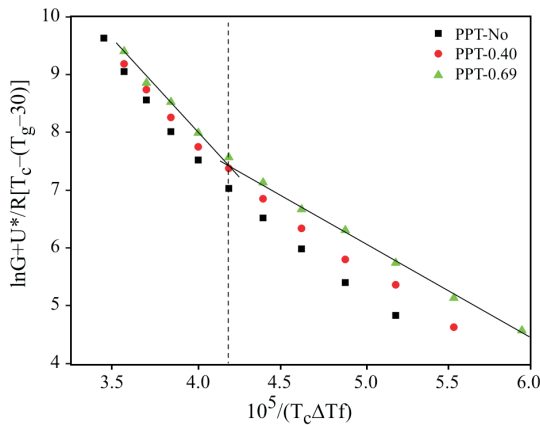


Fig. 5 Lauritzen–Hoffman type plots of the three PPT samples obtained from PLM measurements ($U^*=17590 \text{ J mol}^{-1}$)

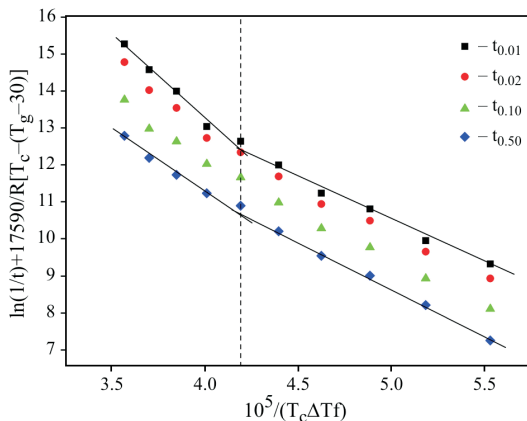


Fig. 6 Lauritzen–Hoffman type plots for PPT-0.69 using the approximation $G \approx 1/t$ and different characteristic crystallisation times

the critical break point denoting a regime III→II transition is clearly observed only when the characteristic times $t_{0.02}$, or $t_{0.01}$ are used. The usual assumption $G \approx 1/t_{1/2}$ result in a slight break point which was not detectable in [7] and [12]. The values of the nucleation parameters calculated before and after this temperature, as well as their ratio are illustrated in Table 3. As it is obvious a ratio $K_{g(III)}/K_{g(II)}$ in the vicinity of the theoretical value 2 is only observed when the characteristic time to achieve 2 or 1% relative crystallinity is used. Given the greater uncertainty in the values when the $t_{0.01}$ is used, it is proposed that the best practice is to use the assumption $G \approx 1/t_{0.02}$.

Finally, it was examined if it would be a good approximation to replace the growth rate, G , with the microscopically measured, from DSC, overall crystallisation rate at 50% relative degree of crystallinity, $(dX/dt)_{X=0.5}$. In Fig. 7, a Lauritzen–Hoffman type plot is illustrated using the above approximation. As it is obvious almost a straight line was observed denoting

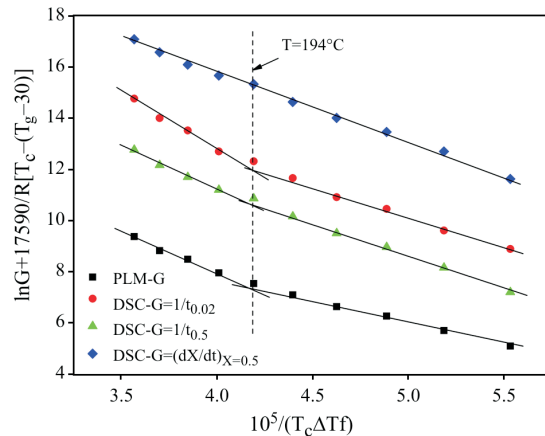


Fig. 7 Lauritzen–Hoffman type plots of PPT-0.69 using different experimental methods

no regime transition in the specific temperature interval. The values of the nucleation parameters calculated assuming a regime transition at the previously reported temperature of 194°C are included in Table 3. The ratio of $K_{g(III)}/K_{g(II)}$ is nearly equal to 1 verifying the almost continuous straight line observed. In Fig. 7, the results obtained using PLM and DSC measurements (with the characteristic times to achieve 50 and 2% relative degree of crystallinity) are also included for comparison reasons. It can be stated that PLM measurements can be resembled only if G is set equal to the inverse characteristic time to achieve 2% relative degree of crystallinity.

Conclusions

Crystallisation kinetics of three poly(propylene terephthalate) samples was examined using PLM and DSC. At low crystallisation temperatures mature spherulites were observed within short experimental times. However, axialitic morphology was noticed at high crystallisation temperatures. The commonly used assumption that the growth rate, G , in the Lauritzen–Hoffman equation can be replaced by the inverse half crystallisation time was critically examined. Based on identical PLM and DSC experiments it can be stated that the best practice is to use the inverse of the crystallisation time to achieve 2% relative degree of crystallinity in place of G .

References

- 1 J. D. Hoffman, G. T. Davis and J. I. Lauritzen Jr., in: N. B. Hannay (Ed.), *Treatise on Solid State Chemistry*, Vol. 3, Plenum Press, New York 1976, Chapter 7.
- 2 J. D. Hoffman and R. L. Miller, *Polymer*, 38 (1997) 3151.
- 3 S. Vyazovkin, J. Stone and N. Sbirrazzuoli, *J. Therm. Anal. Cal.*, 80 (2005) 177.
- 4 M. Avella, S. Cosco, M. L. Di Lorenzo, E. Di Pace and M. Errico, *J. Therm. Anal. Cal.*, 80 (2005) 131.
- 5 T. W. Chan and A. I. Isayev, *Polym. Eng. Sci.*, 34 (1994) 461.
- 6 X. F. Lu and J. N. Hay, *Polymer*, 42 (2001) 9423.
- 7 N. Dangseeyun, P. Shrimoan, P. Supaphol and M. Nithitanakul, *Thermochim. Acta*, 409 (2004) 63.
- 8 M. Mucha and Z. Krolkowski, *J. Therm. Anal. Cal.*, 74 (2003) 549.
- 9 G. Z. Papageorgiou, D. S. Achilias, D. N. Bikiaris and G. P. Karayannidis, *Thermochim. Acta*, 427 (2005) 117.
- 10 S. Vyazovkin and N. Sbirrazzuoli, *Macromol. Rapid Commun.*, 25 (2004) 733.
- 11 G. P. Karayannidis, C. Roupakias, D. N. Bikiaris and D. S. Achilias, *Polymer*, 44 (2003) 931.
- 12 D. S. Achilias, G. Z. Papageorgiou and G. P. Karayannidis, *J. Polym. Sci., Part B: Polym. Phys.*, 42 (2004) 3775.
- 13 M. L. Williams, R. F. Landel and J. D. Ferry, *J. Am. Chem. Soc.*, 77 (1955) 3701.
- 14 P.-D. Hong, W.-T. Chung and C.-F. Hsu, *Polymer*, 43 (2002) 3335.
- 15 J.-M. Huang and F.-C. Chang, *J. Polym. Sci., Part B: Polym. Phys.*, 38 (2000) 934.

Received: August 1, 2005

Accepted: January 30, 2006

OnlineFirst: June 27, 2006

DOI: 10.1007/s10973-005-7260-0